ELSEVIER

Biophysical Chemistry 129 (2007) 172–180

Biophysical Chemistry

http://www.elsevier.com/locate/biophyschem

Effect of structural transition of the host assembly on dynamics of a membrane-bound tryptophan analogue

Ajuna Arora-Sharawat, Amitabha Chattopadhyay *

Centre for Cellular and Molecular Biology, Uppal Road, Hyderabad 500 007, India

Received 28 April 2007; received in revised form 25 May 2007; accepted 28 May 2007
Available online 6 June 2007

Abstract

Tryptophan octyl ester (TOE) represents an important model for membrane-bound tryptophan residues. In this article, we have explored the effect of sphere-to-rod transition of sodium dodecyl sulfate micelles on the dynamics of the membrane-bound tryptophan analogue, TOE, utilizing a combination of fluorescence spectroscopic approaches which include red edge excitation shift (REES). Our results show that REES and fluorescence spectroscopic parameters such as lifetime, anisotropy and acrylamide quenching of micelle-bound TOE are sensitive to the change in micellar organization accompanied by the sphere-to-rod transition.
© 2007 Published by Elsevier B.V.

Keywords: Tryptophan octyl ester; SDS; REES; Sphere-to-rod transition; Ionization state

1. Introduction

Tryptophan residues serve as intrinsic, site-specific fluorescence probes for protein structure and dynamics. The role of tryptophan residues in the structure and function of membrane proteins and peptides has attracted considerable attention. Membrane-spanning proteins are reported to have a significantly higher tryptophan content than soluble proteins [1,2]. It has been observed that tryptophan residues in integral membrane proteins and peptides are not uniformly distributed and that they tend to be localized toward the membrane interface [3]. Statistical studies of sequence databases and available crystal structures of integral membrane proteins also show preferential clustering of tryptophan residues at the membrane interface [4,5]. Furthermore, tryptophan has been found to be an efficient anchor at the membrane interface for transmembrane peptides and proteins [1,2]. The tryptophan-rich aromatic belt at the membrane interface in transmembrane helices is thought to stabilize the helix with respect to the membrane environment [4]. This aromatic belt has also been proposed as a means of directing and stabilizing structural changes during conformational transitions within the transmembrane regions of integral membrane proteins [6]. Importantly, the role of tryptophan residues in maintaining the structure and function of membrane proteins is exemplified by the fact that substitution or deletion of tryptophans often results in reduction or loss of protein functionality [7].

The analysis of fluorescence from multitryptophan proteins is often complicated because of the complexity of fluorescence processes in such systems, and the heterogeneity in fluorescence parameters (such as quantum yield and lifetime) due to the environmental sensitivity of individual tryptophans. Use of suitable model systems could prove to be helpful in such cases. In spite of the importance of membrane-bound tryptophan residues, very few model systems have been developed that could help understand the behavior of tryptophan residues in the membrane. Tryptophan octyl ester (TOE, see Fig. 1) has been recognized as an important model for membrane-bound tryptophan residues. The fluorescence characteristics of TOE incorporated into model membranes and membrane-mimetic systems have been shown to be similar to that of membrane-bound tryptophans [8–12].

Micelles are used as membrane mimetic systems to characterize membrane proteins and peptides [13]. Micelles are highly cooperative, organized molecular assemblies of amphiphiles and are dynamic in nature. Further, they offer certain inherent advantages in fluorescence studies over membranes since micelles

Abbreviations: CMC, critical micelle concentration; REES, red edge excitation shift; SDS, sodium dodecyl sulfate; TOE, tryptophan octyl ester.

* Corresponding author. Tel.: +91 40 2719 2578; fax: +91 40 2716 0311.
E-mail address: amit@ccmb.res.in (A. Chattopadhyay).

0301-4622/$ - see front matter © 2007 Published by Elsevier B.V.
doi:10.1016/j.bpc.2007.05.017

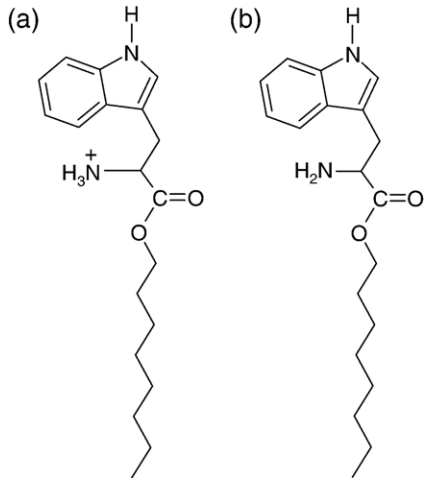

Fig. 1. Chemical structures of (a) protonated and (b) deprotonated forms of TOE.

are smaller and optically transparent, have well-defined sizes, and are relatively scatter-free. Structural transition can be induced in charged micelles at a given temperature by increasing ionic strength of the medium or amphiphile concentration [14]. For example, spherical micelles of sodium dodecyl sulfate (SDS) that exist in water at concentrations higher than critical micelle concentration (CMC) assume an elongated rod-like structure in presence of high electrolyte (salt) concentrations when interactions among the charged headgroups are attenuated due to the added salt (see inset in Fig. 2). This is known as sphere-to-rod transition [15]. This shape change induced by increased salt concentration is accompanied by a reduction in CMC [16]. It has been suggested that large rod-shaped micelles are better models for biomembranes [17] and the hydrocarbon chains are more ordered in rod-shaped micelles compared to spherical micelles [14] giving rise to higher microviscosity in rod-shaped micelles [18]. Micellar sphere-to-rod transitions can be explained in terms of the packing model described by Israelachvili [19]. In this paper, we have explored the effect of sphere-to-rod transition of SDS micelles on the organization and dynamics of the membrane-bound tryptophan analogue, TOE, utilizing a combination of fluorescence spectroscopic approaches.

2. Materials and methods

2.1. Materials

SDS and TOE were purchased from Sigma Chemical Co. (St. Louis, MO, U.S.A.). The purity of SDS was checked by measuring its CMC and comparing with literature CMC. CMC of SDS was determined fluorimetrically utilizing the enhancement of DPH fluorescence upon micellization [16]. The purity of TOE was confirmed as previously reported [9] by thin layer chromatography on precoated silica gel plates in *n*-hexane/methanol/diethyl ether/acetic acid (80:25:20:1,v/v/v/v), and it gave a single spot with both ninhydrin as well as Ehrlich spray. Ultra pure grade acrylamide was from Invitrogen Life Technologies (Carlsbad, CA, U.S.A.). The purity of acrylamide was checked from its absorbance using its molar extinction coefficient (ε) of 0.23$M^{-1}cm^{-1}$ at 295nm and optical transparency beyond 310nm [20]. All other chemicals used were of the highest purity available. Water was purified through a Millipore (Bedford, MA, U.S.A.) Milli-Q system and used throughout.

2.2. Sample preparation

The concentration of SDS (16mM) used was double its CMC (except the REES experiments where it was 48mM), to ensure that it is in the micellar state in all experiments. The molar ratio of TOE/detergent was carefully chosen to give optimum signal-to-noise ratio with minimal perturbation to the micellar organization and negligible interprobe interactions. The maximum molar ratio of TOE/SDS used was 1:120 (mol/mol). At such TOE to detergent ratio, not more than one TOE molecule would be present per micelle on an average, which rules out any TOE aggregation effects [21]. To incorporate TOE into micelles, TOE from methanol stock solution was dried under a stream of nitrogen while being warmed gently (~ 35°C). After further drying under a high vacuum for at least 3h, 1.5ml of 16mM (or 48mM for REES measurements) SDS was added, followed by addition of NaCl (final concentration 0.5M) in case of rod-shaped micelles, and samples were vortexed for 3min. The buffers used were 5mM acetate (pH 5), MOPS (pH 6 and 7), Tris (pH 8 and 9), CAPS (pH 10-12). Background samples were prepared in the similar way except that TOE was omitted from them. All samples were equilibrated at room temperature (~ 23°C) in the dark for 1h.

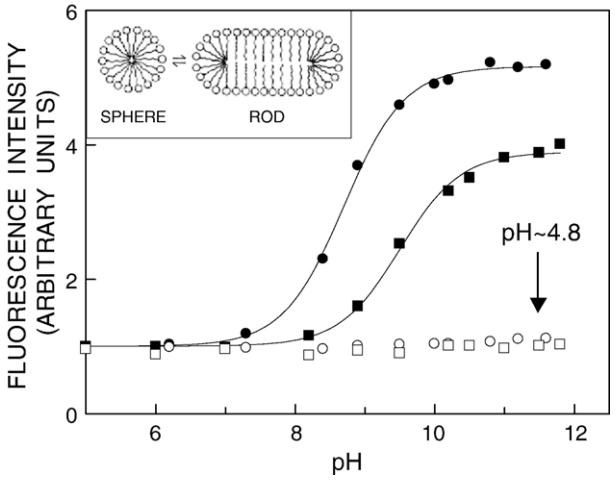

Fig. 2. Effect of sphere-to-rod transition of SDS micelles on ionization state of micelle-bound TOE. Representative data for fluorescence intensity of TOE in SDS micelles in the absence (■) and presence (●) of 0.5 M NaCl as a function of pH are shown. The excitation wavelength used was 280 nm and emission was monitored at 340 nm. The ratio of TOE/SDS was 1:800 (mol/mol) in all cases. Reversibility of fluorescence intensity upon acidification of higher pH samples of TOE in SDS micelles in the absence (□) and presence (○) of 0.5 M NaCl is also shown. Sample pH was lowered by addition of aliquots of 1 M acetic acid and fluorescence was immediately measured. After pH reversal, the samples had a pH of 4.8±0.1. See Materials and methods section for other details. The inset shows a schematic representation of the sphere-to-rod transition in charged SDS micelles induced by salt (adapted from ref. [17]). Note that the headgroup spacing is reduced in rod-shaped micelles due to attenuation of interactions among the charged headgroups by the added salt.

2.3. Steady state fluorescence measurements

Steady state fluorescence measurements were performed with a Hitachi F-4010 spectrofluorometer using 1cm path length quartz cuvettes. Excitation and emission slits with a nominal bandpass of 5nm were used for all measurements. Background intensities of samples in which the fluorophore (TOE) was omitted were negligible in most cases and were subtracted from each sample spectrum to cancel out any contribution due to the solvent Raman peak and other scattering artifacts. The spectral shifts obtained with different sets of samples were identical in most cases, or were within ± 1nm of the ones reported. Fluorescence anisotropy measurements were performed using a Hitachi polarization accessory. Anisotropy values were calculated from the equation [22]:

$$r = \frac{I_{VV} - GI_{VH}}{I_{VV} + 2GI_{VH}} \quad (1)$$

where I_{VV} and I_{VH} are the measured fluorescence intensities (after appropriate background subtraction) with the excitation polarizer vertically oriented and the emission polarizer vertically and horizontally oriented, respectively. G is the grating correction factor and is equal to I_{HV}/I_{HH}. All experiments were done with multiple sets of samples and average values of fluorescence anisotropy are shown in Table 4.

2.4. Time-resolved fluorescence measurements

Fluorescence lifetimes were calculated from time-resolved fluorescence intensity decays using a Photon Technology International (London, Western Ontario, Canada) LS-100 luminescence spectrophotometer in the time-correlated single photon counting mode. This machine uses a thyratron-gated nanosecond flash lamp filled with nitrogen as the plasma gas (17 ± 1 inches of mercury vacuum) and is run at 18–20kHz. Lamp profiles were measured at the excitation wavelength using Ludox (colloidal silica) as the scatterer. To optimize the signal-to-noise ratio, 10,000 photon counts were collected in the peak channel. The excitation wavelength used was 297nm and emission was set at 335 and 345nm for charged and neutral form of TOE, respectively. All experiments were performed using excitation and emission slits with a bandpass of 10nm or less. The sample and the scatterer were alternated after every 5% acquisition to ensure compensation for shape and timing drifts occurring during the period of data collection. This arrangement also prevents any prolonged exposure of the sample to the excitation beam thereby avoiding any possible photodamage to the fluorophore. The data stored in a multichannel analyzer was routinely transferred to an IBM PC for analysis. Fluorescence intensity decay curves so obtained were deconvoluted with the instrument response function and analyzed as a sum of exponential terms:

$$F(t) = \sum\nolimits_i \alpha_i \exp(-t/\tau_i) \quad (2)$$

where $F(t)$ is the fluorescence intensity at time t and α_i is a pre-exponential factor representing the fractional contribution to the time-resolved decay of the component with a lifetime τ_i that $\Sigma_i \alpha_i = 1$. The decay parameters were recovered using a non-linear least squares iterative fitting procedure based on the Marquardt algorithm [23]. The program also includes statistical and plotting subroutine packages [24]. The goodness of the fit of a given set of observed data and the chosen function was evaluated by the reduced χ^2 ratio, the weighted residuals [25], and the autocorrelation function of the weighted residuals [26]. A fit was considered acceptable when plots of the weighted residuals and the autocorrelation function showed random deviation about zero with a minimum χ^2 value not more than 1.4. Mean (average) lifetimes $<\tau>$ for biexponential decays of fluorescence were calculated from the decay times and pre-exponential factors using the following equation [22]:

$$<\tau> = \frac{\alpha_1\tau_1^2 + \alpha_2\tau_2^2}{\alpha_1\tau_1 + \alpha_2\tau_2} \quad (3)$$

2.5. Fluorescence quenching measurements

Acrylamide quenching experiments of TOE fluorescence were carried out by measurement of fluorescence intensity after serial addition of small aliquots of a freshly prepared stock solution of 2M acrylamide in water to a stirred sample followed by incubation for 3min in the sample compartment in the dark (shutters closed). The excitation wavelength used was 295nm and emission was monitored at 335nm and 345nm for samples at pH 5 and pH 11, respectively. Correction for inner filter effect were made using the following equation [22]:

$$F = F_{obs}\text{antilog}[(A_{ex} + A_{em})/2] \quad (4)$$

where F is the corrected fluorescence intensity and F_{obs} is the background subtracted fluorescence intensity of the sample (also corrected for dilution). A_{ex} and A_{em} are the measured absorbances at the excitation and emission wavelengths. The absorbances of the samples were measured using a Hitachi U-2000 UV-visible absorption spectrophotometer. Quenching data were analyzed by fitting to the Stern-Volmer equation [22]:

$$F_o/F = 1 + K_{SV}[Q] = 1 + k_q\tau_o[Q] \quad (5)$$

where F_o and F are the fluorescence intensities in the absence and presence of the quencher, respectively, $[Q]$ is the molar quencher concentration and K_{SV} is the Stern-Volmer quenching constant. The Stern-Volmer constant K_{SV} is equal to $k_q\tau_o$ where k_q is the bimolecular quenching constant and τ_o is the lifetime of the fluorophore in the absence of quencher.

3. Results

3.1. Determination of ionization state of TOE in SDS micelles

TOE fluorescence is known to be sensitive to pH [9]. We utilized this property of TOE fluorescence to follow the ionization of TOE in micelles. Fig. 2 shows the effect of pH on the fluorescence intensity of TOE in SDS micelles in the absence and presence of 0.5M NaCl. In SDS micelles without NaCl, there is a steady increase in fluorescence intensity up to pH 11 after being

Table 1
Fluorescence emission maximum of TOE in SDS micelles

Host	Fluorescence emission maximum[a] (nm)
(A) pH 5	
SDS micelles	335
SDS micelles (in presence of 0.5 M NaCl)	332
(B) pH 11	
SDS micelles	345
SDS micelles (in presence of 0.5 M NaCl)	343

[a] The excitation wavelength was 280 nm. See Materials and methods section for other details.

constant up to pH 8. In case of SDS micelles in the presence of 0.5M NaCl, there is a steady increase in fluorescence intensity up to pH 10, after being constant up to pH 7. It is well established, from studies of the pH dependence of the fluorescence of tryptophan and its derivatives, that in compounds with an amino group in the vicinity of the indole ring, fluorescence is more quenched when the amino group is protonated [27]. We therefore interpret the pH-dependent change in TOE fluorescence as indicative of the deprotonation of the α-amino group of tryptophan in micelle-bound TOE. In other words, the increase in TOE fluorescence with increasing pH can be attributed to the release of the quenching effect of TOE fluorescence with deprotonation of the α-amino group at higher pH. If this change in TOE fluorescence corresponds to deprotonation, it should be reversible. This was tested by the addition of acetic acid permitting fast equilibration of internal and external pH. Fig. 2 shows that these changes in fluorescence intensity are indeed reversible thereby confirming that the observed fluorescence change was due to deprotonation. The apparent pK_a for the α-amino group of the micelle-bound TOE, obtained from Fig. 2, is 9.5 in the absence of salt and 8.7 in the presence of salt. This difference of 0.8 units in the pK_a of TOE indicates different microenvironments experienced by the fluorophore in these two cases. More importantly, the knowledge of pK_a is helpful in selecting a suitable pH in which TOE exists predominantly in the protonated or the deprotonated form (see Fig. 1). This is important since a homogeneous population of fluorophores avoids complications arising from ground state heterogeneity. We therefore chose to work at pH 5 (where TOE would be predominantly protonated) and 11 (deprotonated) for the subsequent experiments.

3.2. Fluorescence and red edge excitation shift of TOE in SDS micelles

Table 1 shows the maximum of fluorescence emission[1] of TOE in SDS micelles at pH 5 and 11 in the absence and presence of salt (representative spectra are shown in Fig. 3). There is a red shift of 10nm in the maximum of fluorescence emission of TOE in SDS micelles (from 335 to 345nm) upon increasing the pH from 5 to 11 corresponding to the deprotonation of TOE. This is similar to what was observed in case of TOE in model membranes [9]. Interestingly, there is a blue shift of 2–3nm in the maximum of fluorescence emission (from 335 to 332nm, and 345 to 343nm) upon addition of salt at both pH, indicating a decrease in polarity in the environment around the tryptophan moiety brought about by the transition of the micelle shape from spherical to rod-like. This is possibly due to a reduction in water content as a result of tighter packing in rod-shaped micelles owing to neutralization of the charge on detergent headgroups by the counterions.

Red edge excitation shift (REES) represents a powerful approach which can be used to directly monitor the environment and dynamics around a fluorophore in a complex biological system [2,28]. A shift in the wavelength of maximum fluorescence emission toward higher wavelengths, caused by a shift in the excitation wavelength toward the red edge of the absorption band, is termed REES. This effect is mostly observed with polar fluorophores in motionally restricted media such as viscous solutions or condensed phases where the dipolar relaxation time for the solvent shell around a fluorophore is comparable to or longer than its fluorescence lifetime [2,28,29]. REES arises from slow rates of solvent relaxation (reorientation) around an excited state fluorophore which depends on the motional restriction imposed on the solvent molecules in the immediate vicinity of the fluorophore. Utilizing this approach, it becomes possible to probe the mobility parameters of the environment itself (which is represented by the relaxing solvent molecules) using the fluorophore merely as a reporter group. Further, since the ubiquitous solvent for biological systems is water, the information obtained in such cases will come from the otherwise 'optically silent' water molecules. The unique feature about REES is that while all other fluorescence techniques (such as fluorescence quenching, energy transfer, and anisotropy measurements) yield information about the fluorophore (either intrinsic or extrinsic) itself, REES provides information about the relative rates of solvent (water in biological systems) relaxation dynamics which is not possible to obtain by other techniques. This makes REES extremely useful since hydration plays a crucial modulatory role in a large number of important cellular events including protein folding, lipid-protein interactions and ion transport [30].

The shifts in the maxima of fluorescence emission of TOE in SDS micelles as a function of excitation wavelength are shown in Fig. 4. As the excitation wavelength is changed from 280 to 302nm (307nm in case of pH 11), the emission maxima of TOE are shifted toward longer wavelengths in all cases. At pH 5, the emission maximum is shifted from 335 to 339nm in case of TOE in spherical micelles, which corresponds to a REES of 4nm. Such dependence of the emission maximum on excitation wavelength is characteristic of REES. This implies that the tryptophan moiety of TOE is localized in a motionally restricted region of the SDS micelle. It is possible that there could be further red shift if excitation is carried out beyond 302nm. We found it difficult to work in this wavelength range due to low signal-to-noise ratio and artifacts due to the solvent Raman peak that sometimes remained even after

[1] We have used the term maximum of fluorescence emission in a somewhat wider sense here. In every case, we have monitored the wavelength corresponding to maximum fluorescence intensity, as well as the center of mass of the fluorescence emission. In most cases, both these methods yielded the same wavelength. In cases where minor discrepancies were observed, the center of mass of emission has been reported as the fluorescence maximum.

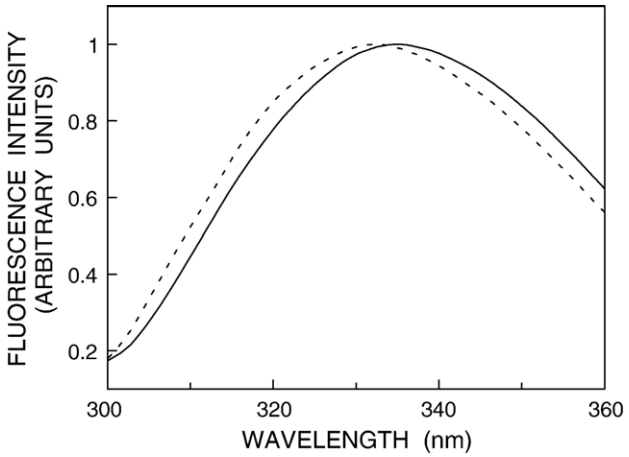

Fig. 3. Representative fluorescence emission spectra of TOE in SDS micelles at pH 5 in the absence (—) and presence (- - -) of 0.5 M NaCl. The excitation wavelength was 280 nm. The ratio of TOE/SDS was 1:120 (mol/mol). See Materials and methods section for other details.

background subtraction. At pH 11, the emission maximum is shifted from 345 to 349nm for TOE in spherical micelles as the excitation wavelength is changed from 280 to 307nm, which corresponds to a REES of 4nm. We have previously shown that when bound to membranes, the tryptophan moiety of TOE is localized in a motionally restricted interfacial region of the membrane and exhibits REES [9]. Thus, the observation of REES for TOE bound to SDS micelles would imply that the tryptophan moiety of TOE is in the interfacial region of the SDS micelles, and this region offers considerable restriction to the reorientational motion of the solvent molecules (dipoles) around the excited state fluorophore. In the presence of 0.5M NaCl (*i.e.*, in the rod-shaped micelles), the emission maximum of TOE exhibits a shift from 332 to 338nm (at pH 5) as the excitation wavelength is changed from 280 to 302nm, corresponding to a REES of 6nm. The observed REES of TOE is therefore influenced by the organization and packing of the constituent amphiphiles such that an increased REES is observed in rod-like micelles. At pH 11, the emission maximum is shifted from 343 to 348nm in case of TOE in rod-like micelles (*i.e.*, in presence of 0.5M NaCl) in response to the change in excitation wavelength from 280 to 307nm, which corresponds to a REES of 5nm.

3.3. Fluorescence lifetime of TOE in SDS micelles

Fluorescence lifetime serves as a sensitive indicator of the local environment in which a given fluorophore is placed [31]. In addition, it is known that the fluorescence lifetime of tryptophan is sensitive to solvent, temperature and excited state interactions [27,32]. A typical decay profile of TOE in SDS micelles at pH 11 with its biexponential fitting and the various statistical parameters used to check the goodness of the fit is shown in Fig. 5. The fluorescence lifetimes of TOE in SDS micelles obtained in the absence and presence of salt are shown in Table 2. As seen from the table, all fluorescence decays could be fitted well with a biexponential function. We chose to use the mean fluorescence lifetime as an important parameter for describing the behavior of TOE in SDS micelles since it is independent of the number of exponentials used to fit the time-resolved fluorescence decay. The mean fluorescence lifetimes of TOE in SDS micelles calculated using Eq. (3) are shown in Table 2. Mean fluorescence lifetime of TOE appears to be higher at pH 11, irrespective of the presence of salt. This is in agreement with earlier results in which it was shown that mean fluorescence lifetime of TOE bound to membranes is increased with increasing pH [9]. The shortening of lifetime at lower pH could signify a change in hydration since tryptophan lifetimes are known to be reduced with an increase in water content of the surrounding medium [32]. Alternatively, the shortening of lifetime at pH 5 could also be due to the cation–π interaction between the positively charged amino group and the indole aromatic ring. Such interaction has previously been implicated in fluorescence quenching and reduction in fluorescence lifetime [33]. Interestingly, the lifetime of TOE in rod-like micelles is more compared to what was observed for TOE in spherical micelles, irrespective of pH. Since the hydrocarbon chains in rod-shaped micelles are more ordered, water penetration is relatively reduced as compared to spherical micelles. In other words, the spherical micelles would allow more water penetration into the micellar interior (see acrylamide quenching results below) and this could lead to a reduction in tryptophan lifetime [32].

3.4. Acrylamide quenching of TOE in SDS micelles

Acrylamide quenching of tryptophan fluorescence is widely used to monitor tryptophan environments in proteins [34]. Fig. 6 shows representative Stern-Volmer plots of acrylamide quenching of TOE in spherical and rod-shaped micelles at pH 5 and 11. The slope (K_{SV}) of such a plot is related to the accessibility (degree of exposure) of the tryptophan moiety to the quencher. The quenching parameters obtained by analyzing the Stern-Volmer plot are shown in Table 3. At pH 5, the Stern–Volmer constant (K_{SV}) for acrylamide quenching of TOE in SDS micelles was found to be 6.37 M^{-1} in the absence of salt while the value of K_{SV} in the presence of salt was found to be 4.40 M^{-1}. At pH 11, the value of K_{SV} for TOE in SDS micelles in the absence of salt was

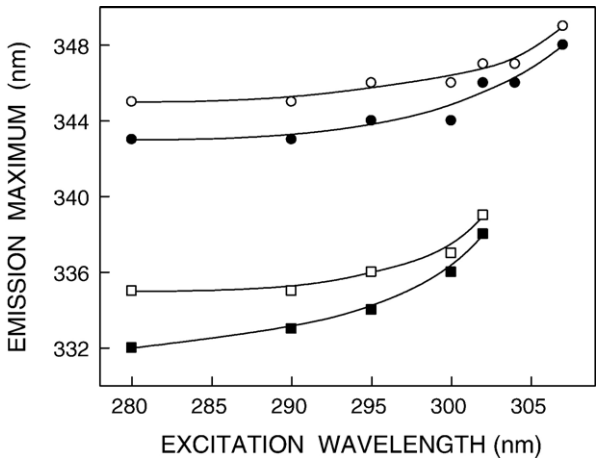

Fig. 4. Effect of changing excitation wavelength on the wavelength of maximum emission of TOE in SDS micelles: pH 5 in the absence (□) and presence (■) of 0.5 M NaCl, and pH 11 in the absence (○) and presence (●) of 0.5 M NaCl. The ratio of TOE/SDS was 1:120 for pH 5 and 1:160 (mol/mol) for pH 11 samples. See Materials and methods section for other details.

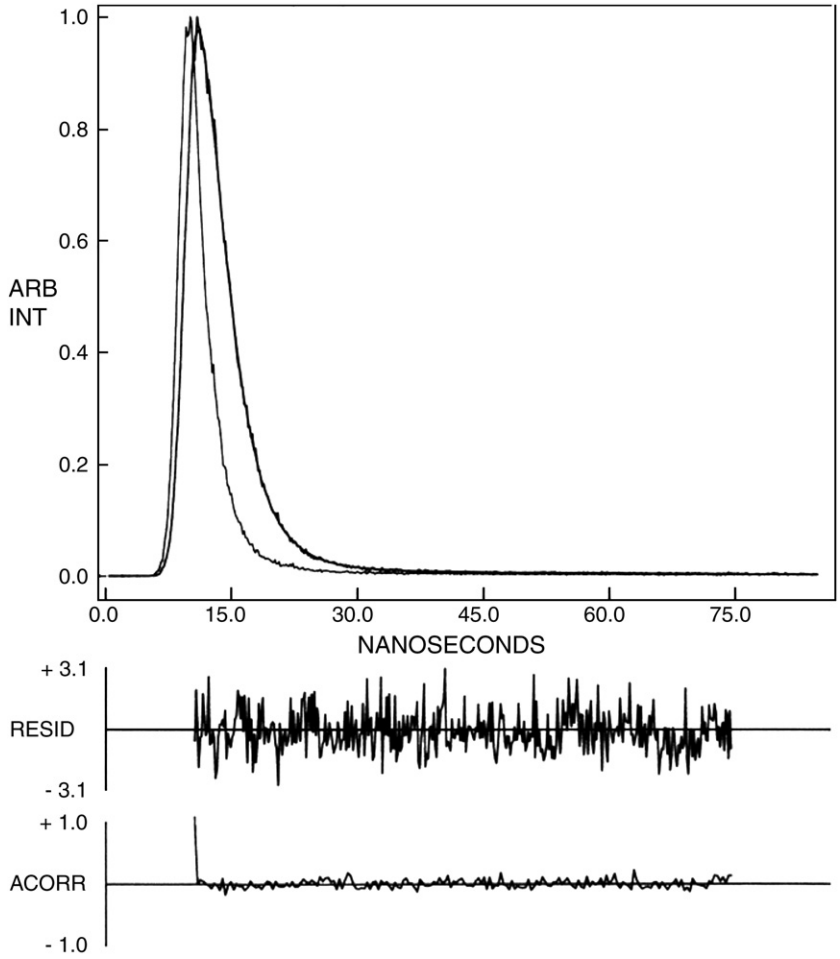

Fig. 5. Time-resolved fluorescence intensity decay of TOE in SDS micelles at pH 11. Excitation wavelength was 297 nm, which corresponds to a peak in the spectral output of the nitrogen lamp. Emission was monitored at 345 nm. The sharp peak on the left is the lamp profile. The relatively broad peak on the right is the decay profile, fitted to a biexponential function. The two lower plots show the weighted residuals and the autocorrelation function of the weighted residuals. The ratio of TOE/SDS was 1:213 (mol/mol). See Materials and methods section for other details.

found to be 16.72 M^{-1} while the value in the presence of salt was found to be 12.52 M^{-1}. However, interpretation of the Stern-Volmer constant is complicated this way due to its intrinsic dependence on fluorescence lifetime (see Eq. (5)). The bimolecular quenching constant (k_q) for acrylamide quenching is therefore a more accurate measure of the degree of exposure since k_q takes into account differences in fluorescence lifetime. The bimolecular quenching constants, calculated using Eq. (5), are shown in Table 3. The k_q values show that the tryptophan moiety of TOE in SDS spherical micelles (in the absence of salt) are considerably more accessible to acrylamide, relative to that in rod-shaped micelles (in presence of salt). This could be a result of reduced water penetration (and therefore reduced accessibility to the aqueous quencher acrylamide) in the more tightly packed rod-shaped micelles formed in the presence of NaCl.

3.5. Fluorescence anisotropy and apparent rotational correlation time

The steady state fluorescence anisotropy of TOE in SDS micelles is shown in Table 4. As seen in the table, at pH 5, fluorescence anisotropy for TOE is higher in SDS micelles in the presence of salt. At pH 11 however, the fluorescence anisotropy for TOE in SDS micelles in the presence and absence of salt remains the same. In order to correct for any lifetime-induced artifact in fluorescence anisotropy, the apparent (average)

Table 2
Fluorescence lifetimes of TOE in SDS micelles[a]

Host	α_1	τ_1 (ns)	α_2	τ_2 (ns)	$\langle\tau\rangle$[b] (ns)
(A) pH 5					
SDS Micelles	0.96	0.54	0.04	2.78	0.94
SDS Micelles (in presence of 0.5 M NaCl)	0.97	0.76	0.03	3.82	1.17
(B) pH 11					
SDS Micelles	0.90	2.03	0.10	3.89	2.36
SDS Micelles (in presence of 0.5 M NaCl)	0.81	2.23	0.19	3.82	2.69

[a] The excitation wavelength was 297 nm; emission was monitored at 335 and 345 nm for pH 5 and 11, respectively. The ratio of TOE/SDS was 1:133 for pH 5 and 1:213 (mol/mol) for pH 11 samples. See Materials and methods section for other details.

[b] Calculated using Eq. (3).

Table 3
Acrylamide quenching of TOE in SDS micelles [a]

Host	K_{SV} [b] (M^{-1})	k_q ($\times 10^{-9}$) [c] ($M^{-1}s^{-1}$)
(A) pH 5		
SDS micelles	6.37±0.19	6.78
SDS micelles (in presence of 0.5 M NaCl)	4.40±0.22	3.76
(B) pH 11		
SDS micelles	16.72±0.40	7.08
SDS micelles (in presence of 0.5 M NaCl)	12.52±0.47	4.65

[a] The ratio of TOE/SDS was 1:213 for pH 5 and 1:800 (mol/mol) for pH 11 samples. The excitation wavelength was 295 nm; emission was monitored at 335 and 345 nm for pH 5 and 11, respectively. See Materials and methods section for other details.
[b] Calculated using Eq. (5). The quenching parameter shown represents the means±S.E. of at least three independent measurements while quenching data shown in Fig. 6 are from representative experiments.
[c] Calculated using mean fluorescence lifetimes from Table 2 and using Eq. (5).

Table 4
Fluorescence anisotropy of TOE in SDS micelles [a]

Host	Fluorescence anisotropy [b]	τ_c [c] (ns)
(A) pH 5		
SDS micelles	0.057	0.52
SDS micelles (in presence of 0.5 M NaCl)	0.065	0.80
(B) pH 11		
SDS micelles	0.022	0.38
SDS micelles (in presence of 0.5 M NaCl)	0.022	0.43

[a] The excitation wavelength was 280 nm; emission was monitored at 335 nm and 345 nm for pH 5 and 11, respectively. The ratio of TOE/SDS was 1:400 for pH 5 and 1:800 (mol/mol) for pH 11 samples. See Materials and methods section for other details.
[b] Calculated using Eq. (1). The values shown are the means of three independent measurements.
[c] Calculated using Eq. (6). See text for other details.

rotational correlation times for TOE in micelles were calculated using Perrin's equation [22]:

$$\tau_c = \frac{<\tau> r}{r_o - r} \quad (6)$$

where r_o is the limiting anisotropy of tryptophan, r is the steady state anisotropy, and $<\tau>$ is the mean fluorescence lifetime taken from Table 2. Although Perrin's equation is not strictly applicable to this system, it is assumed that this equation will apply to a first approximation, especially because we have used mean fluorescence lifetimes for the analysis of multiple component lifetimes. The values of the apparent rotational correlation times, calculated this way using a value of r_o of 0.16 [35], are shown in Table 4. The rotational correlation times are lower at pH 11 compared to values at pH 5, possibly due to motional restriction caused by charge interactions at pH 5 where TOE exists in the protonated form and/or a change in probe location. Both at pH 5 and 11, the rotational correlation time of TOE appears to be longer in rod-shaped micelles indicating that rotational motion is faster in spherical micelles. Interestingly, the anisotropy and rotational correlation times for TOE in rod-shaped micelles closely resemble the corresponding values for TOE in membrane bilayers [9] thereby reinforcing the fact that rod-shaped micelles are more representative of membrane bilayers [17].

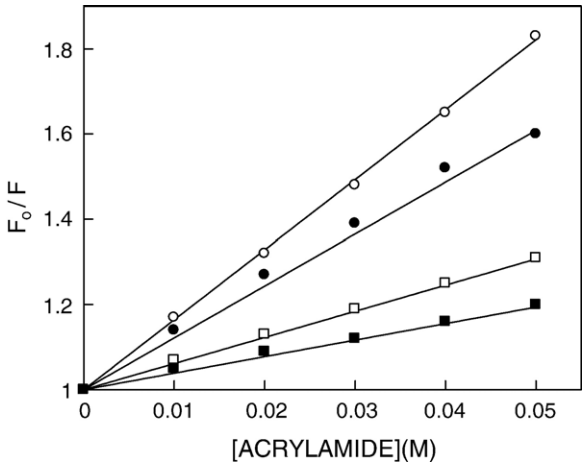

Fig. 6. Representative data for Stern-Volmer analysis of acrylamide quenching of TOE fluorescence in SDS micelles: pH 5 in the absence (□) and presence (■) of 0.5 M NaCl, and pH 11 in the absence (○) and presence (●) of 0.5 M NaCl. F_o is the fluorescence in the absence of quencher, and F is the corrected fluorescence in the presence of quencher. The excitation wavelength was fixed at 295 nm and emission was monitored at 335 nm and 345 nm for samples at pH 5 and 11, respectively. The ratio of TOE/SDS was 1:213 for pH 5 and 1:800 (mol/mol) for pH 11 samples. See Materials and methods section for other details.

4. Discussion

Structural transitions involving shape changes play an important role in cellular physiology. For example, the shape of erythrocytes (red blood cells) has been shown to change with the pH and ionic strength of the medium [36]. The shape of the erythrocyte is thought to be maintained by the membrane skeleton in close interaction with the plasma membrane [37]. Investigations into the role of the membrane in such shape changes have revealed that modification of either the membrane composition or the structure of its individual constituents can lead to shape changes [38]. Thus, alteration of the cholesterol composition, selective removal of phospholipids from the outer membrane leaflet, pH and membrane potential alterations, metabolic depletion, and introduction of lysophospholipids, fatty acids, and charged amphipathic agents in membranes leads to shape changes in erythrocytes [38–40]. Shape changes can be induced even in liposomes by mechanical stress, temperature or pH variation, osmotic shock, and by asymmetric transmembrane distribution of phospholipids [41]. Shape changes in cellular membranes that occur due to modifications of membrane composition [38–40] can directly affect the function of membrane proteins such as mechanosensitive channels that respond to changes in membrane curvature [42]. For example, the function of the gramicidin channel has been shown to be sensitive to curvature changes of the membrane bilayer [43]. Interestingly, SDS micellar shape change induced by chlorpromazine, an amphiphilic cationic phenothiazine drug, has recently been reported [44].

In this paper, we have examined shape changes associated with the salt-induced sphere-to-rod structural transition in charged micellar assemblies by monitoring changes in fluorescence of micelle-bound TOE, a model for tryptophan residues in membranes. We report here that REES of micelle-bound TOE is enhanced in rod-like micelles. This is possibly due to the fact that micelles are intrinsically more dynamic than membranes and the organization and packing of amphiphiles in rod-like micelles are similar to that of a membrane bilayer. The difference in organization of spherical and rod-shaped micelles is also apparent from differences in fluorescence anisotropy and lifetime, along with accessibility monitored by acrylamide quenching measurements. These results could have implications for membrane proteins and peptides. For example, it has been recently reported that the conformation and dynamics of the ion channel gramicidin is sensitive to structural changes in the host assembly [45]. Taken together, our results show that REES, in combination with other fluorescence parameters, offer a sensitive approach to monitor structural changes in organized molecular assemblies. These results could be significant in changes in membrane morphology observed under certain physiological conditions.

Acknowledgements

This work was supported by the Council of Scientific and Industrial Research, Government of India. A.A.S. thanks the Life Sciences Research Board for the award of a Project Assistantship. We thank Y.S.S.V. Prasad and G.G. Kingi for technical help, Devaki Kelkar for helpful discussions, and Puneet Sharawat, Yamuna Devi Paila, Md. Jafurulla, and Sandeep Shrivastava for help during the preparation of the manuscript. We thank members of our laboratory for critically reading the manuscript. A.C. is an Honorary Professor of the Jawaharlal Nehru Centre for Advanced Scientific Research, Bangalore (India).

References

[1] M. Schiffer, C.H. Chang, F.J. Stevens, The functions of tryptophan residues in membrane proteins, Protein Eng. 5 (1992) 213–214.
[2] H. Raghuraman, D.A. Kelkar, A. Chattopadhyay, Novel insights into membrane protein structure and dynamics utilizing the red edge excitation shift, in: C.D. Geddes, J.R. Lakowicz (Eds.), Reviews in Fluorescence 2005, vol. 2, Springer, New York, 2005, pp. 199–222.
[3] D.A. Kelkar, A. Chattopadhyay, Membrane interfacial localization of aromatic amino acids and membrane protein function, J. Biosci. 31 (2006) 297–302.
[4] R.A.F. Reithmeier, Characterization and modeling of membrane proteins using sequence analysis, Curr. Opin. Struck. Biol. 5 (1995) 491–500.
[5] M.B. Ulmschneider, M.S.P. Sansom, Amino acid distributions in integral membrane protein structures, Biochim. Biophys. Acta 1512 (2001) 1–14.
[6] C. Domene, S. Vemparala, M.L. Klein, C. Venien-Bryan, D.A. Doyle, Role of aromatic localization in the gating process of a potassium channel, Biophys. J. 90 (2006) L01–L03.
[7] M.D. Becker, D.V. Greathouse, R.E. Koeppe, O.S. Andersen, Amino acid sequence modulation of gramicidin channel function: effects of tryptophan-to-phenylalanine substitutions on the single-channel conductance and duration, Biochemistry 30 (1991) 8830–8839.
[8] A.S. Ladokhin, P.W. Holloway, Fluorescence of membrane-bound tryptophan octyl ester: a model for studying intrinsic fluorescence of protein-membrane interactions, Biophys. J. 69 (1995) 506–517.
[9] A. Chattopadhyay, S. Mukherjee, R. Rukmini, S.S. Rawat, S. Sudha, Ionization, partitioning, and dynamics of tryptophan octyl ester: implications for membrane-bound tryptophan residues, Biophys. J. 73 (1997) 839–849.
[10] B. de Foresta, J. Gallay, J. Sopkova, P. Champeil, M. Vincent, Tryptophan octyl ester in detergent micelles of dodecylmaltoside: fluorescence properties and quenching by brominated detergent analogs, Biophys. J. 77 (1999) 3071–3084.
[11] B. Sengupta, P. Sengupta, Influence of reverse micellar environments on the fluorescence emission properties of tryptophan octyl ester, Biochem. Biophys. Res. Commun. 277 (2000) 13–19.
[12] A. Chattopadhyay, A. Arora, D.A. Kelkar, Dynamics of a membrane-bound tryptophan analog in environments of varying hydration: a fluorescence approach, Eur. Biophys. J. 35 (2005) 62–71.
[13] D.S. Dijkstra, J. Broos, A.J.W.G. Visser, A. van Hoek, G.T. Robillard, Dynamic fluorescence spectroscopy on single tryptophan mutants of EII (mtl) in detergent micelles. Effects of substrate binding and phosphorylation on the fluorescence and anisotropy decay, Biochemistry 36 (1997) 4860–4866.
[14] H. Heerklotz, A. Tsamaloukas, K. Kita-Tokarczyk, P. Strunz, T. Gutberlet, Structural, volumetric, and thermodynamic characterization of a micellar sphere-to-rod transition, J. Am. Chem. Soc. 126 (2004) 16544–16552.
[15] P.J. Missel, N.A. Mazer, M.C. Carey, G.B. Benedek, Thermodynamics of the sphere-to-rod transition in alkyl sulfate micelles, in: K.L. Mittal, E.J. Fendler (Eds.), Solution Behavior of Surfactants: Theoretical and Applied Aspects, vol. 1, Plenum Press, New York, 1982, pp. 373–388.
[16] A. Chattopadhyay, E. London, Fluorimetric determination of critical micelle concentration avoiding interference from detergent charge, Anal. Biochem. 139 (1984) 408–412.
[17] S.S. Rawat, A. Chattopadhyay, Structural transition in the micellar assembly: a fluorescence study, J. Fluoresc. 9 (1999) 233–244.
[18] B. Jönsson, B. Lindman, K. Holmberg, B. Kronberg, Surfactants and Polymers in Aqueous Solution, John Wiley, New York, 1998.
[19] J.N. Israelachvili, Intermolecular and Surface Forces, 2nd edition. Academic Press, London, 1991.
[20] M.R. Eftink, Fluorescence Quenching Reactions: Probing Biological Macromolecular Structure, in: T.G. Dewey (Ed.), Biophysical and biochemical aspects of fluorescence spectroscopy, Plenum Press, New York, 1991, pp. 1–41.
[21] A. Helenius, K. Simons, Solubilization of membranes by detergents, Biochim. Biophys. Acta 415 (1975) 29–79.
[22] J.R. Lakowicz, Principles of Fluorescence Spectroscopy, 3rd edition. Springer, New York, 2006.
[23] P.R. Bevington, Data Reduction and Error Analysis for the Physical Sciences, McGraw-Hill, New York, 1969.
[24] D.V. O'Connor, D. Phillips, Time-Correlated Single Photon Counting, Academic Press, London, 1984, pp. 180–189.
[25] R.A. Lampert, L.A. Chewter, D. Phillips, D.V. O'Connor, A.J. Roberts, S.R. Meech, Standards for nanosecond fluorescence decay time measurements, Anal. Chem. 55 (1983) 68–73.
[26] A. Grinvald, I.Z. Steinberg, On the analysis of fluorescence decay kinetics by the method of least-squares, Anal. Biochem. 59 (1974) 583–598.
[27] J.M. Beechem, L. Brand, Time-resolved fluorescence of proteins, Ann. Rev. Biochem. 54 (1985) 43–71.
[28] A. Chattopadhyay, Exploring membrane organization and dynamics by the wavelength-selective fluorescence approach, Chem. Phys. Lipids 122 (2003) 3–17.
[29] A.P. Demchenko, The red-edge effects: 30 years of exploration, Luminescence 17 (2002) 19–42.
[30] P. Mentré (Ed.), Water in the cell, Cell. Mol. Biol., vol. 47, 2001, pp. 709–970.
[31] F.G. Prendergast, Time-resolved fluorescence techniques: methods and applications in biology, Curr. Opin. Struct. Biol. 1 (1991) 1054–1059.
[32] E.P. Kirby, R.F. Steiner, The influence of solvent and temperature upon the fluorescence of indole derivatives, J. Phys. Chem. 74 (1970) 4480–4490.
[33] A.J. Weaver, M.D. Kemple, J.W. Brauner, R. Mendelsohn, F.G. Prendergast, Fluorescence, CD, attenuated total reflectance (ATR) FTIR, and 13C NMR characterization of the structure and dynamics of synthetic

melittin and melittin analogues in lipid environments, Biochemistry 31 (1992) 1301–1311.
[34] M.R. Eftink, Fluorescence quenching: theory and applications, in: J.R. Lakowicz (Ed.), Topics in Fluorescence Spectroscopy, vol. 2, Plenum Press, New York, 1991, pp. 53–126.
[35] M.R. Eftink, L.A. Selvidge, P.R. Callis, A.A. Rehms, Photophysics of indole derivatives: experimental resolution of L_a and L_b transitions and comparison with theory, J. Phys. Chem. 94 (1990) 3469–3479.
[36] M. Rasia, A. Bollini, Red blood cell shape as a function of medium's ionic strength and pH, Biochim. Biophys. Acta 1372 (1998) 198–204.
[37] E.J. Luna, A.L. Hitt, Cytoskeleton-plasma membrane interactions, Science 258 (1992) 955–963.
[38] F.A. Kuypers, B. Roelofsen, W. Berendsen, J.A.F. Op den Kamp, L.L.M. van Deenen, Shape changes in human erythrocytes induced by replacement of the native phosphatidylcholine with species containing various fatty acids, J. Cell. Biol. 99 (1984) 2260–2267.
[39] L. Backman, J.B. Jonasson, P. Hörstedt, Phosphoinositide metabolism and shape control in sheep red blood cells, Mol. Membr. Biol. 15 (1998) 27–32.
[40] M.M. Gedde, W.H. Huestis, Membrane potential and human erythrocyte shape, Biophys. J. 72 (1997) 1220–1233.
[41] E. Farge, P.F. Devaux, Shape changes of giant liposomes induced by an asymmetric transmembrane distribution of phospholipids, Biophys. J. 61 (1992) 347–357.
[42] E. Perozo, A. Kloda, D.M. Cortes, B. Martinac, Physical principles underlying the transduction of bilayer deformation forces during mechanosensitive channel gating, Nat. Struct. Biol. 9 (2002) 696–703.
[43] J.A. Lundbaek, A.M. Maer, O.S. Andersen, Lipid bilayer electrostatic energy, curvature stress, and assembly of gramicidin channels, Biochemistry 36 (1997) 5695–5701.
[44] W. Caetano, E.L. Gelamo, M. Tabak, R. Itri, Chlorpromazine and sodium dodecyl sulfate mixed micelles investigated by small angle X-ray scattering, J. Colloid Interface Sci. 248 (2002) 149–157.
[45] S.S. Rawat, D.A. Kelkar, A. Chattopadhyay, Effect of structural transition of the host assembly on dynamics of an ion channel peptide: a fluorescence approach, Biophys. J. 89 (2005) 3049–3058.